Gomisin A enhances the antitumor effect of paclitaxel by suppressing oxidative stress in ovarian cancer

TAIWEI WANG[1,2*], JIAN LIU[1*], XUEMIAO HUANG[2], CHUANQI ZHANG[1], MENGYUAN SHANGGUAN[1], JUNYU CHEN[1], SHAN WU[3], MENGMENG CHEN[2], ZHAOYUN YANG[2] and SHUHUA ZHAO[1]

[1]Department of Gynaecology and Obstetrics, The Second Hospital, Jilin University, Changchun, Jilin 130021; [2]Department of Rehabilitation, School of Nursing, Jilin University, Changchun, Jilin 130022; [3]Department of Reproductive Endocrinology, Women's Hospital, Zhejiang University, School of Medicine, Hangzhou, Zhejiang 310006, P.R. China

Received March 31, 2022; Accepted August 30, 2022

DOI: 10.3892/or.2022.8417

Abstract. Gomisin A (GA) is an effective component of *Schisandra*. The crude extracts of *Schisandra chinensis* and its active ingredients have been shown to inhibit multidrug resistance in tumour cells. Reactive oxygen species (ROS) have different roles in cancer and may contribute to therapy resistance. The human ovarian cancer (OC) cell lines SKOV3 and A2780, and a mouse model of OC, were used in the present study. MTT assay, colony formation assay, flow cytometry, western blot analysis, and haematoxylin and eosin (H&E) staining were performed to determine the antitumor effect of GA and paclitaxel (PTX) *in vitro* and *in vivo*. The ROS inhibitor N-acetyl cysteine (NAC) was used to assess the mechanism underlying the chemosensitizing effects of GA. Notably, the proliferation of OC cells was inhibited by PTX, which could be enhanced by the ROS inhibitor NAC or GA. Treatment with NAC + PTX or GA + PTX enhanced the cell cycle arrest, but not apoptosis, induced by PTX. Moreover, the molecular mechanism underlying this effect may be that GA decreases the levels of ROS in ovarian cancer cells and inhibits cell cycle progression by downregulating the expression of the cell cycle proteins cyclin-dependent kinase 4 and cyclin B1. In conclusion, the combination of PTX and the ROS inhibitor GA may be a novel strategy in OC chemotherapy.

Correspondence to: Professor Shuhua Zhao, Department of Gynaecology and Obstetrics, The Second Hospital, Jilin University, 218 Ziqiang Street, Changchun, Jilin 130022, P.R. China
E-mail: zhaoshuhua-1966@163.com

*Contributed equally

Abbreviations: GA, Gomisin A; FS, Fructus Schizandra; ROS, reactive oxygen species; PTX, paclitaxel; NAC, N-acetyl cysteine; OC, ovarian cancer; DMSO, dimethyl sulfoxide; DHE, dihydroethidium; MMP-2, matrix metallopeptidase 2; CDKs, cyclin-dependent kinases

Key words: GA, OC, ROS, PTX, chemosensitization

Introduction

Ovarian cancer (OC) is a type of gynaecological malignant tumour and is the eighth leading cause of cancer-associated mortality in women worldwide (1). The high mortality rate associated with OC may be due to its late detection, as the vast majority of patients with OC are diagnosed at an advanced stage (2), and thus encounter recurrence and drug resistance. Although a significant proportion of patients with advanced disease can achieve a complete response with tumour resection and adjuvant chemotherapy, the majority of patients will relapse within 2 years (2,3). The 5-year survival rate of patients with advanced OC is ~40% in the United States (4,5). The combination of paclitaxel (PTX) and carboplatin is the first-line medication for postoperative treatment in patients with OC. PTX can bind to tubulin proteins and enhance their polymerization to induce mitotic G_2/M phase arrest, which results in cell cycle arrest (6). However, PTX application is limited because of its serious side effects and multidrug resistance in tumour cells (7,8). Over the past decade, there has been little improvement in the cure rate for advanced OC; therefore, it is necessary to develop effective therapeutics to overcome chemoresistance.

In recent years, adjuvant chemotherapy with traditional Chinese medicine has been widely considered. *Schisandra chinensis* is a perennial woody vine of the Magnoliaceae family, which is commonly used as a traditional Chinese medicine. It is commonly called Wuweizi or 'five-flavour fruit' in China. Fructus Schizandra has a high medicinal value because of its protective effect on a number of organs, including the heart, liver, kidney, nervous system and gastrointestinal tract (9). The active ingredient of *Schisandra chinensis*, Schisandrin B, has been used to treat human lung carcinoma cells (10) and murine breast cancer 4T1 cells (11). In addition, it has been demonstrated that the major bioactive constituents of Fructus Schizandra can significantly enhance the doxorubicin-induced apoptosis of cancer cells, such as SMMC7721, a human hepatic carcinoma cell line, and MCF-7, a human breast cancer cell line (12). Crude extracts of *S. chinensis* have been shown to reverse multidrug resistance and improve the sensitivity of cancer

cells to chemotherapeutic drugs by inhibiting the expression of P-glycoprotein and protein kinase C (13). Furthermore, previous studies have indicated that an effective component of *Schisandra*, Gomisin A (GA), serves a role in reversing drug resistance (14), inhibiting proliferation, and exerting anti-oxidant and anti-inflammatory activities (15). In addition, as one of the major bioactive constituents of Fructus Schizandra, GA has been shown to possess anticancer and antiangiogenic activity (16). Although GA has exhibited its inhibitory effects against various tumour cell lines, such as melanoma (17) and colorectal cancer (18) cell lines, its cytotoxicity in OC cells has not yet been evaluated. Furthermore, the benefit of the combination of GA and PTX on OC cells is unknown.

It has previously been reported that PTX can promote the production of reactive oxygen species (ROS) (19). ROS are a series of chemical compounds containing oxygen produced during cellular metabolism, including superoxide anion, hydroxyl radical and hydrogen peroxide; these chemicals can act on lipids, proteins and DNA (20). Oxidative stress induced by potential ROS causes irreversible cell damage and death; however, it has also been suggested that ROS can initiate carcinogenesis and help tumour cells survive (21). Radiation, tobacco and xenobiotics have long been some of the best-known sources of ROS and are associated with tumour-induced events (22). Therefore, the present study hypothesized that GA could enhance the sensitivity of OC cells to PTX by reducing ROS production.

In the present study, the human ovarian cancer cell lines SKOV3 and A2780 were used to investigate the effects of an effective component of *Schisandra*, GA, with PTX *in vitro* and *in vivo*. The present study assessed whether GA could increase the antitumor effects of PTX. Moreover, by observing the changes in ROS in cells, the possible mechanism underlying the effects of GA-induced ROS inhibition on PTX sensitivity was discussed.

Materials and methods

Chemicals and reagents. GA (purity ≥98%), PTX (purity ≥98%), and N-acetyl cysteine (NAC; purity ≥98%) were purchased from Shanghai Yuanye Bio-Technology Co., Ltd. An MTT reagent kit and dimethyl sulfoxide (DMSO) were purchased from MilliporeSigma. Wright-Giemsa stain solution, and haematoxylin and eosin (H&E) Staining Kit were purchased from Beijing Solarbio Science & Technology Co., Ltd. Propidium iodide (PI), RNase-A, Triton X-100, ROS DCFH-DA assay kit (cat. no. S0033S), and radioimmunoprecipitation assay (RIPA) lysis buffer were purchased from Beyotime Institute of Biotechnology. An Annexin V-FITC/PI cell apoptosis detection kit was purchased from Beijing TransGen Biotech Co., Ltd. Dihydroethidium (DHE; cat. no. KGAF019) assay kit was purchased from Nanjing KeyGen Biotech Co., Ltd. Antibodies against epidermal growth factor receptor (EGFR; cat. no. 18986-1-AP), PI3K (cat. no. 20584-1-AP), Akt (cat. no. 10176-2-AP), phosphorylated (p)-Akt (cat. no. 66444-1-Ig), β-actin (cat. no. 20536-1-AP), cyclin-dependent kinase 4 (CDK4; cat. no. 11026-1-AP), cyclin B1 (cat. no. 28603-1-AP), GAPDH (cat. no. 10494-1-AP), matrix metallopeptidase 2 (MMP-2; cat. no. 10373-2-AP), Nrf2 (cat. no. 16396-1-AP), Keap-1 (cat. no. 10503-2-AP), NQO1 (cat. no. 11451-1-AP), and Ki-67 (cat. no. 27309-1-AP) were purchased from Wuhan Sanying Biotechnology.

Cell culture. SKOV3 and A2780 cell lines were obtained from the Prostate Disease Prevention and Control Centre, Basic Medical College of Jilin University; the SKOV3 (cat. no. CL-0215) and A2780 (cat. no. CL-0013) cell lines were originally purchased from Procell Life Science & Technology Co., Ltd. The SKOV3 cells were cultured in Iscove's modified Dulbecco's medium (HyClone; Cytiva) and the A2780 cells were cultured in Dulbecco's modified Eagle's medium (HyClone; Cytiva) both supplemented with 10% foetal bovine serum (Gibco; Thermo Fisher Scientific, Inc.), 100 U/ml penicillin and 100 μg/ml streptomycin at 37˚C in a humidified atmosphere containing 5% CO_2.

Animals. A total of 20 female BALB/c-Nu mice (age, 6 weeks; weight, 16-20 g) were purchased from Beijing Vital River Laboratory Animal Technology Co., Ltd., and were reared under specific pathogen-free conditions at a temperature of 22±1˚C and 45-55% humidity. Mice were maintained under a 12-h light/dark cycle and were provided with *ad libitum* access to food and water. The feeding and handling of experimental animals followed the regulations of Jilin University and the *in vivo* experimental protocol was approved by the Experimental Animal Ethics Committee of Jilin University Second Hospital (approval no. 2018106; Changchun, China).

A2780 cells ($2x10^6$ cells) were subcutaneously injected into the right back of each mouse. When the volume reached 100-150 mm^3, the mice were distributed into four groups (n=5 mice/group) as follows: i) Control group, in which mice were intraperitoneally injected with 200 μl PBS once every 2 days; ii) GA group, in which mice were intraperitoneally injected with 200 μl GA (10 mg/kg) once every 2 days; iii) PTX group, in which mice were intraperitoneally injected with 200 μl PTX (10 mg/kg) once every 2 days; and iv) PTX combined with GA group, in which mice received the same dose of each drug as the monotherapy group. PTX and GA were dissolved in saline. For each mouse, a volume of 200 μl solution containing the drug was injected each time.

Tumour volume was calculated daily as follows: Volume=L x $W^2/2$, where L and W represent the length and width of the tumour, respectively. In addition, the body weight of each mouse was calculated daily. No animals were withdrawn from the study. After 14 days of treatment, the mice were euthanized by cervical dislocation under inhalation of excess ether (mice were anaesthetized until their muscles were completely relaxed and their eyelid reflexes disappeared, the ether was then removed and mice were sacrificed by cervical dislocation), and the tumours were excised and weighed. The heart, liver, spleen, lung and kidney were also removed for further analysis. The specific humane endpoints used to determine euthanasia were when the tumours were >2,000 mm^3, tumour diameter was >20 mm, or body weight loss was >20%. Death was verified by observation of the cessation of breath and heartbeat, and areflexia.

MTT assay. The *in vitro* cytotoxicity of GA, NAC and PTX in SKOV3 and A2780 cells was measured using the MTT assay, as previously described (23). Briefly, the cells were cultured

in 96-well plates at a density of 3,000 cells/well. SKOV3 and A2780 cells were treated with 0.04 μM GA, 16 μg/ml PTX or their combination (GA + PTX group) for 6 and 24 h at 37˚C. In addition, for additional experiments, SKOV3 and A2780 cells were incubated with 0.5 mM NAC for 1 h, and then 16 μg/ml PTX was added to the NAC + PTX group for 6 and 24 h at 37˚C. After being exposed to the drugs, MTT (5 mg/ml) was added to each well. After incubated at 37˚C for 4 h, DMSO was added to dissolve the precipitate. The absorbance of each well was measured the optical density at 490 nm (OD490). All experiments were repeated three times. The inhibition rates were calculated as following: Inhibition rate (%)=(ODc-Odt)/ODc, where ODt and ODc represent the OD490 values of the treatment group and control group, respectively.

Colony formation. SKOV3 and A2780 cells were seeded into 6-well plates at 300 cells/well and were treated with GA, PTX, NAC, NAC + PTX or GA + PTX for 2 weeks at 37˚C. The drug concentrations were the same as those used prior to the MTT assay, and these concentrations were used for the subsequent experiments *in vitro*. After treatment, the cells were fixed with 4% paraformaldehyde for 15 min at 37˚C and washed three times with PBS. Finally, the cells were stained with Wright-Giemsa stain solution according to the manufacturer's protocols. The colonies containing >50 cells were counted. The cell clonality rates were calculated as following: Cell clonality (%)=colony number/seeded cells number.

Cell cycle and apoptosis assays. SKOV3 and A2780 cells were seeded into 6-well plates at 4x10^5 cells/well and were divided into different groups with the indicated treatments for 24 h at 37˚C, after which cell cycle progression and apoptosis were analysed. For the cell cycle assay, after being harvested, the cells were fixed in 70% precooled ethanol overnight at -20˚C and then suspended in PBS containing 50 μg/ml PI, 100 μg/ml RNase-A and 0.2% Triton X-100 for 30 min at 4˚C in the dark. The stained cells were analysed by a FACScan flow cytometer (BD Biosciences), and the results were analysed by Modfit LT 5 software (Verity Software House, Inc.).

For apoptosis detection. all cells, both floating and adherent, were harvested. Subsequently, the cells were stained with 5 μl Annexin V-FITC and 5 μl PI for 15 min at room temperature in the dark according to the manufacturer's instructions. The stained cells were analysed by a FACScan flow cytometer and the results were analysed using BD Diva 3 software (BD Biosciences).

Wound scratch assay and Transwell invasion assay. For the wound scratch assay, SKOV3 and A2780 cells were seeded into 12-well plates at 3x10^5 cells/well. When the cells reached 80-90% confluence, a sterile 200-μl pipette tip was used to scratch the cell monolayer. The wounds were observed at 0 and 48 h after being treated with GA, NAC, PTX, NAC + PTX or GA + PTX in serum-free medium at 37˚C. Cell images were captured by an optical microscope (Motic Incorporation, Ltd.). Semi-quantification of the wound scratch assay was conducted by measuring the gap distance. Migration rate (%) was calculated as follows: (0 h gap distance-48 h gap distance)/0 h gap distance.

For the invasion assay, 24-well Transwell chambers (pore size, 8.0 μm; cat. no. 3422; Corning, Inc.) were used to analyse the invasive ability of the cells in each treatment group. The chamber was coated with Matrigel (BD Biosciences) according to the manufacturer's instructions. A total of 3x10^4 cells/well were seeded into the upper chamber with 100 μl serum-free media-based drugs (0.04 μM GA, 16 μg/ml PTX and 0.5 mM NAC), whereas 600 μl 10% FBS-containing media-based drug was added into the lower chamber. After 24 h of treatment at 37˚C, the chambers were removed and stained with Wright-Giemsa staining solution as aforementioned for colony formation. Images were captured by an optical microscope (Motic Incorporation, Ltd.).

Western blot analysis. Briefly, cells were collected after different treatments and maintained on ice. The cells were resuspended in RIPA lysis buffer, according to the manufacturer's instructions, for protein extraction, and protein concentrations were quantified using the bicinchoninic acid method. Western blot analysis was conducted as previously described (24). A total of 20 μg proteins were loaded per lane into a 4-15% Precast Tris-Glycine Gel (TransGen Biotech Co., Ltd.); the proteins were then separated electrophoretically and transferred to PVDF membranes. The PVDF membranes were blocked with 5% skim milk at room temperature for 30 min, followed by incubation with the primary antibodies overnight at 4˚C. The membranes were then incubated with HRP-tagged goat anti-rabbit and anti-mouse antibodies secondary antibodies (1:10,000; cat. nos. SA00001-2 and SA00001-1; Proteintech Group, Inc.) for 1 h at room temperature. Finally, the bands were visualized using the ECL method (BeyoECL Moon kit; cat. no. P0018FS; Beyotime Institute of Biotechnology) on a ChemiScope 6000 Exp chemiluminescence imaging system (Clinx Science Instruments Co., Ltd.) and were semi-quantified with ImageJ software (Version 2.1.0/1.53c; National Institutes of Health). The following dilutions of primary antibodies were used: Anti-EGFR (1:3,000), anti-PI3K (1:500), anti-Akt (1:5,000), anti-p-Akt (1:5,000), anti-β-actin (1:3,000), anti-CDK4 (1:4,000), anti-cyclin B1 (1:4,000), anti-GAPDH (1:10,000), anti-MMP-2 (1:500), anti-Nrf-2 (1:3,000), anti-Keap-1 (1:5,000) and anti-NQO1 (1:4,000).

DHE staining. Cells were plated into 6-well cell culture plates at a density of 4x10^5 cells/well were treated according to the aforementioned methods. After being washed with PBS twice, the cells were incubated with 2 ml medium containing 10% FBS and 5 μM DHE for 30 min at 37˚C in the dark and were then visualized under a fluorescence microscope (Motic Incorporation, Ltd.). Red staining indicating oxidative stress was semi-quantified (ROS-positive staining) using ImageJ software (Version 2.1.0/1.53c).

DCHF-DA staining. Cells were plated on 6-well cell culture plates at a density of 4x10^5 cells/well and were then treated with GA, NAC, PTX, NAC + PTX, and GA + PTX. All of the cells were harvested in medium supplemented with 10% FBS, centrifuged at 300 x g for 5 min at room temperature, and resuspended in PBS containing 10 μM DCHF-DA. Cells were maintained at 37˚C in the dark for 30 min. Subsequently,

the cells were pelleted by centrifugation at 300 x g for 5 min at room temperature and resuspended in preheated PBS. The cells were finally analysed using a FACScan flow cytometer and the results were analysed by BD Diva 3 software.

Immunohistochemical (IHC) and H&E staining. IHC staining and H&E staining were conducted as previously described (25). Briefly, tumour, heart, liver, spleen, lung and kidney tissues were fixed in 10% formalin at room temperature overnight, embedded in paraffin and then cut into 4-μm consecutive sections. For H&E staining, following deparaffinization and rehydration, the sections were stained with H&E, according to the manufacturer's protocol. Images were captured under an optical microscope (Motic Incorporation, Ltd.). For IHC staining, following deparaffinization and rehydration, the slides were heated in a microwave oven at 97˚C for 20 min with EDTA retrieval buffer (Beijing Solarbio Science & Technology Co., Ltd.) for epitope retrieval. Nonspecific blinding was conducted with PBS containing 2% BSA (cat. no. AR1006; Boster Biological Technology) for 2 h at room temperature. Subsequently, the sections were incubated with anti-Ki-67 (1:6,000), anti-p-Akt (1:200), anti-MMP-2 (1:200) and anti-Nrf2 (1:200) primary antibodies at 4˚C overnight. Slides were then incubated with HRP-conjugated goat anti-rabbit IgG (1:200) and goat anti-Mouse IgG (1:200) secondary antibodies, for 30 min at room temperature, and were then visualized with a DAB Detection Kit (Thermo Fisher Scientific, Inc.). Images were captured under an optical microscope (Motic Incorporation, Ltd.) and were semi-quantified with ImageJ software (Version 2.1.0/1.53c).

Routine blood examination. Whole blood samples (200 μl) were collected from retro-orbital venous sinus of each mouse after inhalation of ether at the final day of the experiment. The white blood cell (WBC) count, red blood cell (RBC) count, haemoglobin (HGB) count and blood platelet (PLT) count were analysed using a haematology analyser (Shinova).

Statistical analysis. All data are presented as the mean ± SD. One-way ANOVA followed by Bonferroni's post hoc test was used for comparisons between multiple groups. All experiments were repeated three times. ANOVA was performed using SPSS (version 26; IBM Corp.) software and graphs were constructed using GraphPad Prism 5 (GraphPad Software, Inc.). $P<0.05$ was considered to indicate a statistically significant difference.

Results

GA enhances the proliferation-inhibiting effect of PTX on OC cells. The structure of GA is shown in Fig. 1A. The inhibitory effects of GA and PTX on two OC cell lines, SKOV3 and A2780, were detected by MTT assay. The results showed that the inhibition rates of SKOV3 and A2780 cells treated with GA + PTX were significantly increased compared with the inhibition rates of the PTX group at 6 and 24 h (Fig. 1B). These data indicated that GA could reinforce the sensitivity of SKOV3 and A2780 cells to PTX. The antioxidant effect of GA has been widely confirmed (26). To identify whether a GA-induced reduction in ROS levels was associated with the inhibition of cell proliferation, GA was replaced with NAC. The MTT results showed that the inhibition rates of SKOV3 and A2780 cells treated with NAC + PTX were almost identical to the inhibition rates of the GA + PTX group. To verify the effect of GA and PTX on the proliferation of OC cells, a colony formation assay was performed (Fig. 1C). Treatment with GA or NAC combined with PTX resulted in a significantly reduced colony formation rate in both OC cell lines compared with that in the PTX group.

To gain insight into the mechanism by which GA enhances the sensitivity of SKOV3 and A2780 cells to PTX, flow cytometry was used to detect the rate of apoptosis (Fig. 1D). The results revealed that apoptotic rate was very similar between the PTX group and both combined groups in both cell lines. The apoptotic rate of the GA + PTX group was significantly increased compared with that in control group in both SKOV3 and A2780 cells, whereas the apoptotic rate of the NAC + PTX group was only increased compared with the control group in SKOV3 cells. These results indicated that the apoptotic process may not be involved in the mechanism by which GA mediates the enhancement of sensitivity to PTX in OC cells.

In addition, to investigate whether the mechanism was related to the cell cycle, PI staining was employed to observe cell cycle progression. According to the results of flow cytometric analysis (Fig. 1E), the treatment of both cell lines with PTX significantly increased the proportion of cells in the G_2/M phase of the cell cycle and decreased the proportion of cells in the G_0/G_1 phase of the cell cycle. In addition, the two combination treatments, GA + PTX and NAC + PTX, enhanced the accumulation of cells in the G_2/M phase compared with PTX treatment alone.

To explore the mechanism underlying the effects of NAC, GA and PTX on G_2/M phase arrest, western blot analysis was performed to measure the expression levels of the cell cycle-regulating proteins cyclin B1 and CDK4. CDK4 has been reported to play an important role in regulating cell G_1, as CDK4 mediates the progression of cells from G_1 to S phase (27), and cyclin B1 regulates the G_2/M phase (28). In the present study, the expression levels of CDK4 in the control, NAC, PTX, NAC + PTX, and GA + PTX groups in both cells and GA group in A2780 cell were consistent with the proportion of cells in G_1 phase, in that the lower the proportion of cells in G_1 phase, the lower the expression of CDK4 detected. However, in the GA group of SKOV3 cells, the proportion of cells in G_1 phase showed no difference with that of the control group, whereas the expression of CDK4 was significantly decreased compared with that in the control group. It was hypothesized that these results were caused by the higher sensitivity of SKOV3 cells to GA than A2780 cells, and that the change in molecular level (CDK4 protein) needed more time to cause a change in the reduction of the proportion of cells in G_1 phase. The expression of cyclin B1 was significantly upregulated following treatment with PTX alone in A2780 cells, but not in SKOV3 cells, and it was hypothesized that these results were associated with the low-dose ROS stimulation produced by PTX. Compared with in the PTX group, the expression levels of cyclin B1 and CDK4 were significantly attenuated in the groups treated with NAC + PTX and GA + PTX (Fig. 2A and C).

In addition, the PI3K/Akt signalling pathway was analysed by western blotting. The situation of cyclin B1 also occurred in the PI3K/AKT pathway. Although PTX downregulated

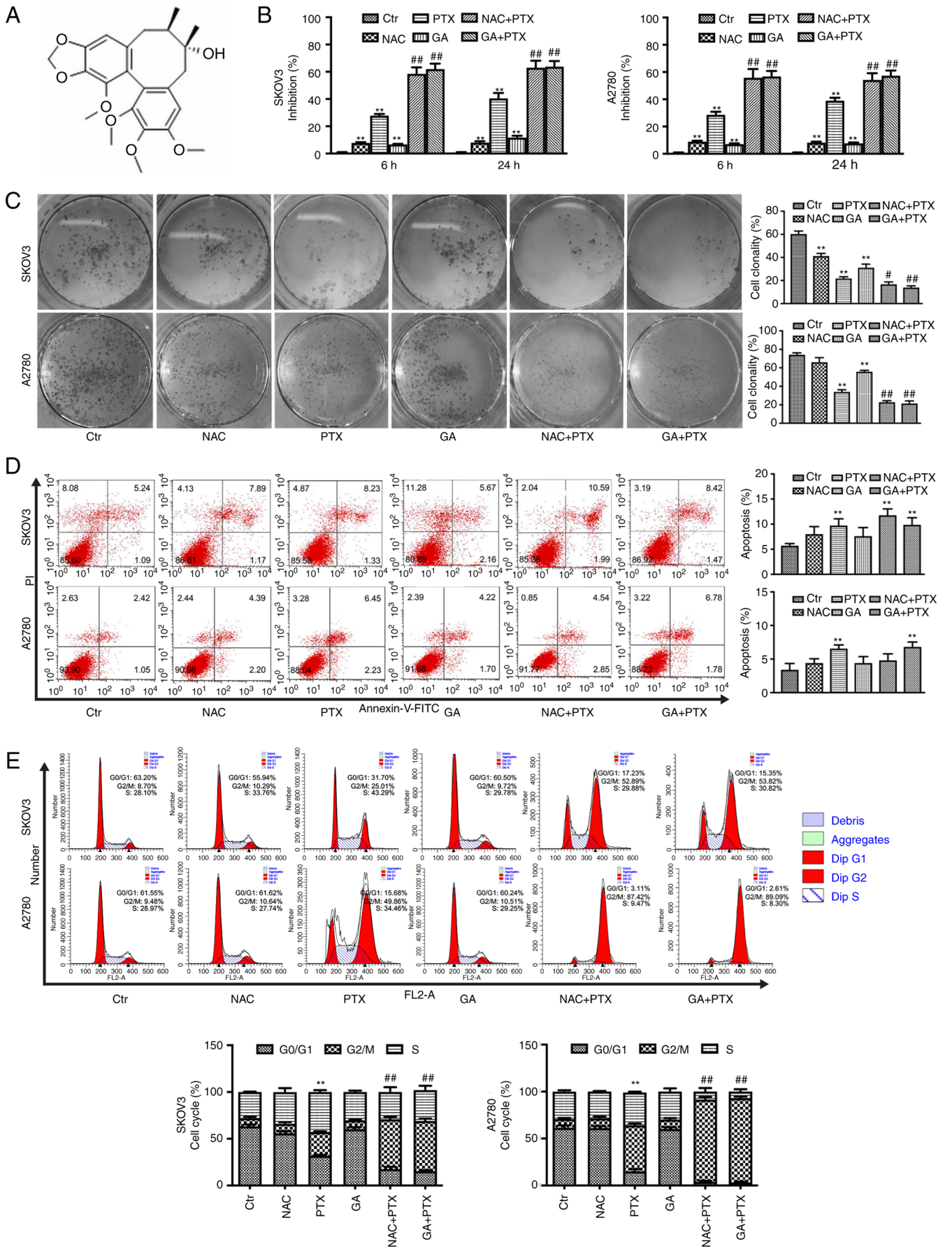

Figure 1. GA enhances the proliferation-inhibiting effect of PTX on ovarian cancer cells. (A) Structure of GA. (B) Inhibitory effects of different treatments on SKOV3 and A2780 cells. (C) Colony formation assay of cell clonality of SKOV3 and A2780 cells. (D) Flow cytometric and statistical analysis of apoptosis. (E) Flow cytometric and statistical analysis of cell cycle progression. Data are expressed as the mean ± SD from three independent experiments. **P<0.01 vs. Ctrl; $^{\#}$P<0.05, $^{\#\#}$P<0.01 vs. PTX. Ctr, control; GA, Gomisin A; NAC, N-acetyl cysteine; PTX, paclitaxel.

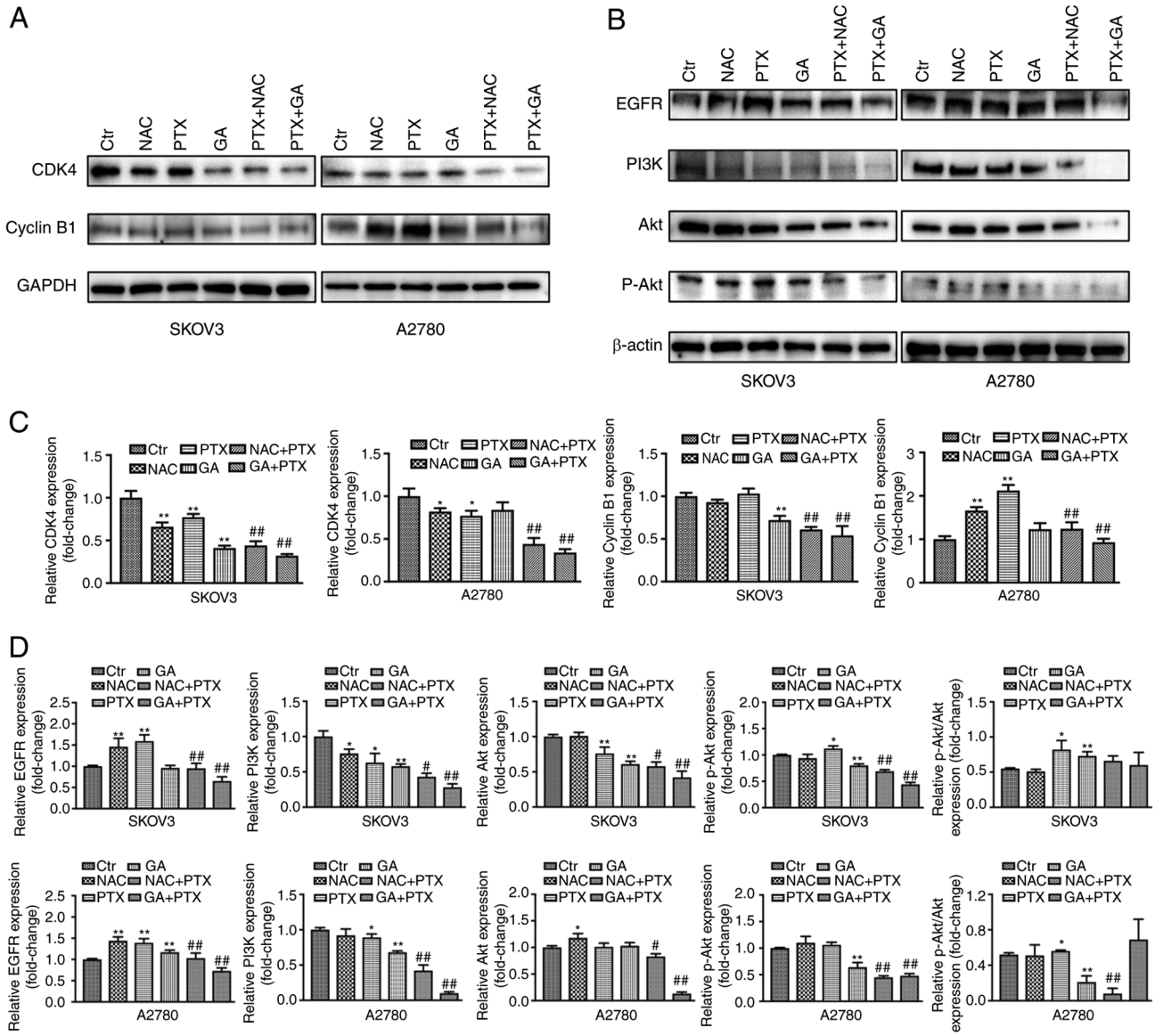

Figure 2. Effects of GA and PTX treatment on protein expression in ovarian cancer cells. Expression levels of (A) CDK4 and cyclin B1, and (B) EGFR, PI3K, Akt and p-Akt were detected by western blotting. (C and D) Semi-quantification of the western blot analysis. Data are expressed as the mean ± SD from three independent experiments. *P<0.05, **P<0.01 vs. Ctrl; $^{\#}$P<0.05, $^{\#\#}$P<0.01 vs. PTX. Ctr, control; EGFR, epidermal growth factor receptor; GA, Gomisin A; NAC, N-acetyl cysteine; p, phosphorylated; PTX, paclitaxel.

the expression levels of PI3K, the low-dose ROS stimulation produced by PTX upregulated the expression levels of p-AKT, which is an important downstream protein of the PI3K pathway. Similarly, the expression levels of PI3K, AKT and p-AKT were downregulated in the NAC + PTX and GA + PTX groups. Subsequently, the ratio of p-Akt/Akt was assessed in each group. The ratio of p-Akt/Akt in the PTX group was significant increased compared with that in the control group. Although there was no difference in the p-Akt/Akt ratio between the PTX group and the GA + PTX group, total Akt was markedly lower in the GA + PTX group, which resulted in a higher ratio of p-Akt/Akt in the GA + PTX group (Fig. 2B and D).

These data suggested that GA and PTX could block the G_2/M phase and induce cell cycle arrest in OC cells, indicating that the inhibitory effect of PTX enhanced by GA was mediated by blocking the cell cycle, but not apoptosis.

GA enhances the inhibitory effects of PTX on OC cell invasion and migration. To clarify whether GA or NAC could increase the inhibitory effects of PTX on SKOV3 and A22780 cell invasion and migration, wound scratch and Transwell invasion assays were used to detect the migration and invasion of both cell lines, respectively. The migratory ability of both SKOV3 and A2780 cells was decreased in the GA, NAC and PTX groups compared with that in the control group. Following treatment with GA + PTX and NAC + PTX, the migratory ability of SKOV3 and A2780 cells was further decreased compared with that in cells treated with PTX or GA alone, and the difference was statistically significant (Fig. 3A and C). Chambers coated with Matrigel were used to mimic the extracellular matrix and simulate the invasion process of tumour cells *in vivo*. The invasion rate, relative to the control group, of SKOV3 and A2780 cells in the GA + PTX treatment groups was significantly lower than

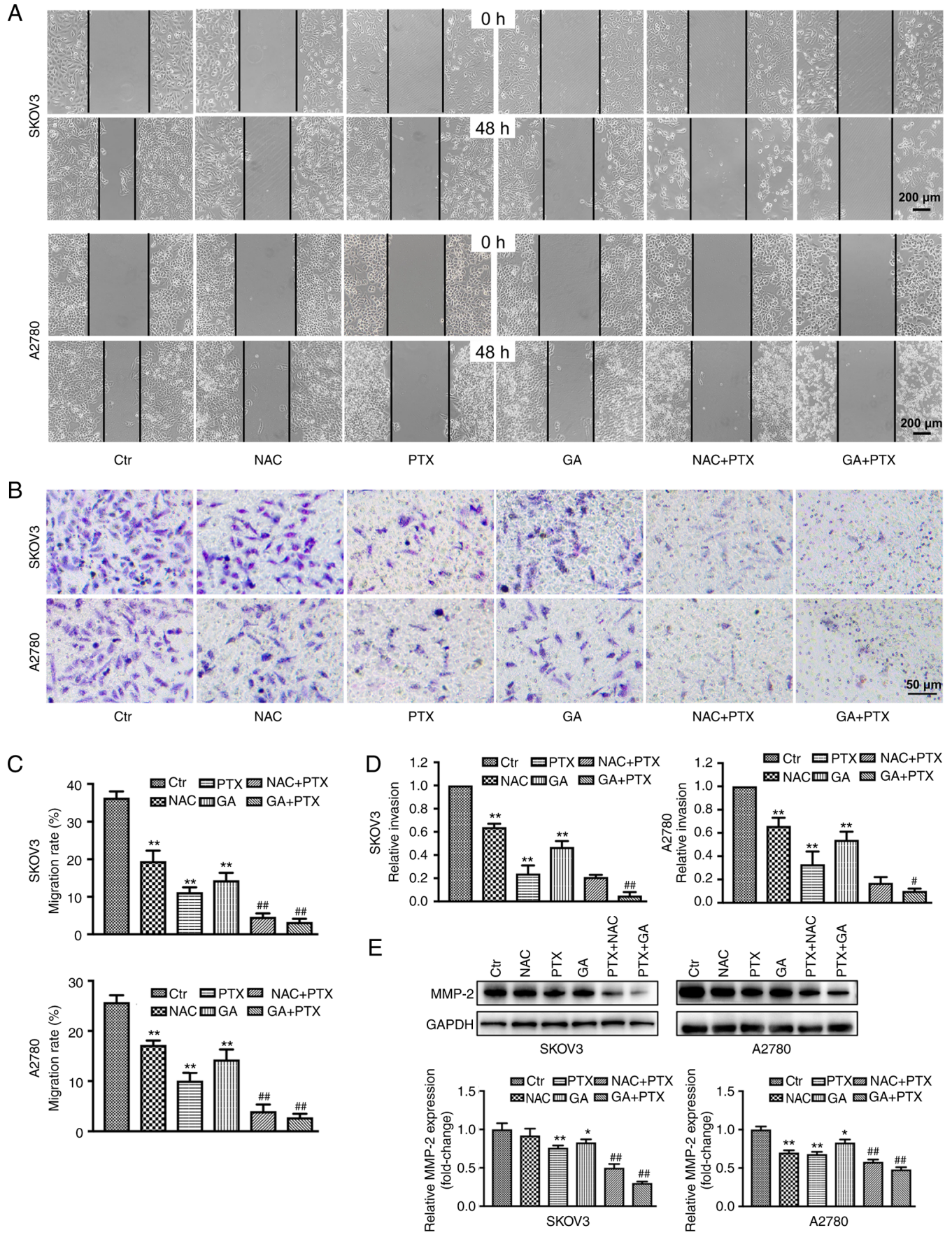

Figure 3. GA enhances the inhibitory effect of PTX on ovarian cancer cell migration and invasion. (A and C) Migratory ability of SKOV3 and A2780 cells following different treatments, as determined by the wound scratch assay. (B and D) Invasive ability of SKOV3 and A2780 cells following different treatments, as determined by Transwell assay. (E) Expression levels of MMP-2, as detected by western blot analysis. Data are expressed as the mean ± SD from three independent experiments. *P<0.05, **P<0.01 vs. Ctrl; $^{\#}$P<0.05, $^{\#\#}$P<0.01 vs. PTX. Ctr, control; GA, Gomisin A; NAC, N-acetyl cysteine; PTX, paclitaxel; MMP-2, matrix metallopeptidase 2.

the relative invasion rate of both SKOV3 and A2780 cells in the PTX group (Fig. 3B and D).

Western blotting results showed that following treatment with NAC + PTX or GA + PTX, the expression levels of MMP-2 were downregulated compared with those in the PTX group (Fig. 3E).

GA enhances the inhibitory effects of PTX on OC cells by downregulating the levels of ROS. As shown in the aforementioned results, the NAC + PTX group exhibited a similar inhibitory effect to the GA + PTX group. To explore whether this was mediated by a GA-induced reduction in ROS levels, ROS were detected by DHE staining. The PTX group exhibited a marked increase in ROS production; ROS levels were presented as fluorescence intensity relative to the control group. However, the relative fluorescence intensity was decreased in the GA + PTX and NAC + PTX groups compared with that in the PTX group (Fig. 4A). In addition, flow cytometry was employed to detect the ROS content in each group. The results were in accordance with the DHE staining results (Fig. 4B and C). Furthermore, the Keap-1/Nrf-2 signalling pathway was detected by western blotting (Fig. 4D). Compared with in the control group, the expression levels of Keap-1 were downregulated in the PTX group, whereas they were upregulated in the GA + PTX and NAC + PTX groups. The expression levels of Nrf-2 and NQO1 were upregulated in the PTX group but were markedly downregulated in the GA + PTX and NAC + PTX groups. These results indicated that GA strengthened the sensitivity of SKOV3 and A2780 cells to PTX, which was mediated by ROS inhibition regulated by GA.

GA enhances the inhibitory effects of PTX on mouse ovarian subcutaneous xenograft tumours. When tumour volume reached 100-150 mm^3, the mice were distributed into each group and the *in vivo* antitumor effect study was initiated. Notably, there was no significant difference in the mean graft volume among the four groups at the start of the study. A direct visual representation of the tumours is shown in Fig. 5A. The suppressive effect of GA on tumour volume and weight was only slightly smaller than that in the control group and no statistically significant difference was observed in terms of antitumor effect, which may be due to the low dose of GA used. By contrast, the PTX group and the combined group exhibited an obvious reduction in tumour growth compared with that in the control group. Moreover, the combination group further enhanced the tumour inhibitory effects of the PTX group.

To further validate the antitumor activity of GA and PTX, pathological analysis of tumour tissues was performed by H&E staining (Fig. 5B). Tumour necrosis was not obvious and most tissue structures were intact in the control group. In the GA, PTX and combined groups, the tumour tissue was impaired to varying degrees, and the pathological differences were noticeable, with nuclei in the necrotic area showing pyknosis and fragmentation, and with some nuclei disappearing.

Immunohistochemical staining was further used to detect the expression of the cell proliferation markers Ki-67 and p-Akt, the cell migration marker MMP-2 and the ROS marker Nrf2 (Fig. 5C and D). The highest Ki-67, MMP-2 and p-Akt expression levels were both detected in the control group of A2780 tumour-bearing mice, whereas the lowest were detected in the combined group. Nrf2 expression was markedly upregulated in the PTX group compared with that in the control group, whereas it was obviously downregulated in the GA and GA + PTX groups; the expression of Nrf2 was much lower in the GA + PTX than that in the GA group. The immunohistochemistry results for Ki-67, p-Akt, MMP-2 and Nrf2 expression were consistent with those of western blot analysis of *in vitro* results.

Additionally, biosafety assessments were performed by H&E staining to detect histological changes in the heart, liver, spleen, lung and kidney (Fig. 6A), and routine blood examinations of WBC, RBC, HGB and PLT (Fig. 6B). The results of H&E staining showed that no obvious pathological damage was detected, and no significant differences were identified in the routine blood examinations of each group.

Discussion

OC is a malignant tumour of the female reproductive system, which is associated with a high mortality rate (29). Platinum-based chemotherapy combined with PTX is the most important adjuvant therapy for OC. Although PTX has strong antiangiogenic activity, the drug resistance of PTX, which may be related to the production of ROS induced by it, limits its clinical application to a certain extent (19). Notably, the antioxidant activity of GA has been widely proven (13) and the present study confirmed this. In recent years, GA has been widely used in several research domains due to its minimal side effects (30,31); however, the exact effect of GA on human OC is unclear. In the present study, OC cells treated with GA or PTX were observed, and the results provided a theoretical and experimental basis for the practical application of PTX-based combined chemotherapy in the clinic.

The sensitivity of OC cells to PTX is based on the growth inhibition rate. Previous studies have shown that EGFR overexpression in a number of solid tumours is associated with tumour cell proliferation, angiogenesis, tumour invasion, metastasis and inhibition of apoptosis (32,33). The present study demonstrated that the expression of EGFR was significantly decreased after GA combined with PTX treatment, indicating that GA + PTX could significantly enhance the inhibition of proliferation of the OC cell lines A2780 and SKOV3 compared with PTX alone. As GA has an antioxidant effect, it was hypothesized that GA could decrease the level of ROS produced by PTX. In addition, a specific inhibitor of ROS, NAC, was used in the present study. As an antioxidant, a high dose of NAC (5 mM) has previously been shown to completely suppress ROS in cells, which could induce cell protection (34). In the present study, low-dose (0.5 mM) NAC only neutralized the ROS that initiated cell proliferation, but did not entirely suppress ROS levels. Additionally, the inhibitory effect of NAC was identified in previous studies (35,36); therefore, NAC was used in the present study to definitively identify whether the enhancement of the sensitivity of OC cells to PTX was related to GA-induced ROS reduction.

An increasing number of studies have reported that ROS can have dual roles, with different doses having different effects. High ROS concentrations inhibit cell survival,

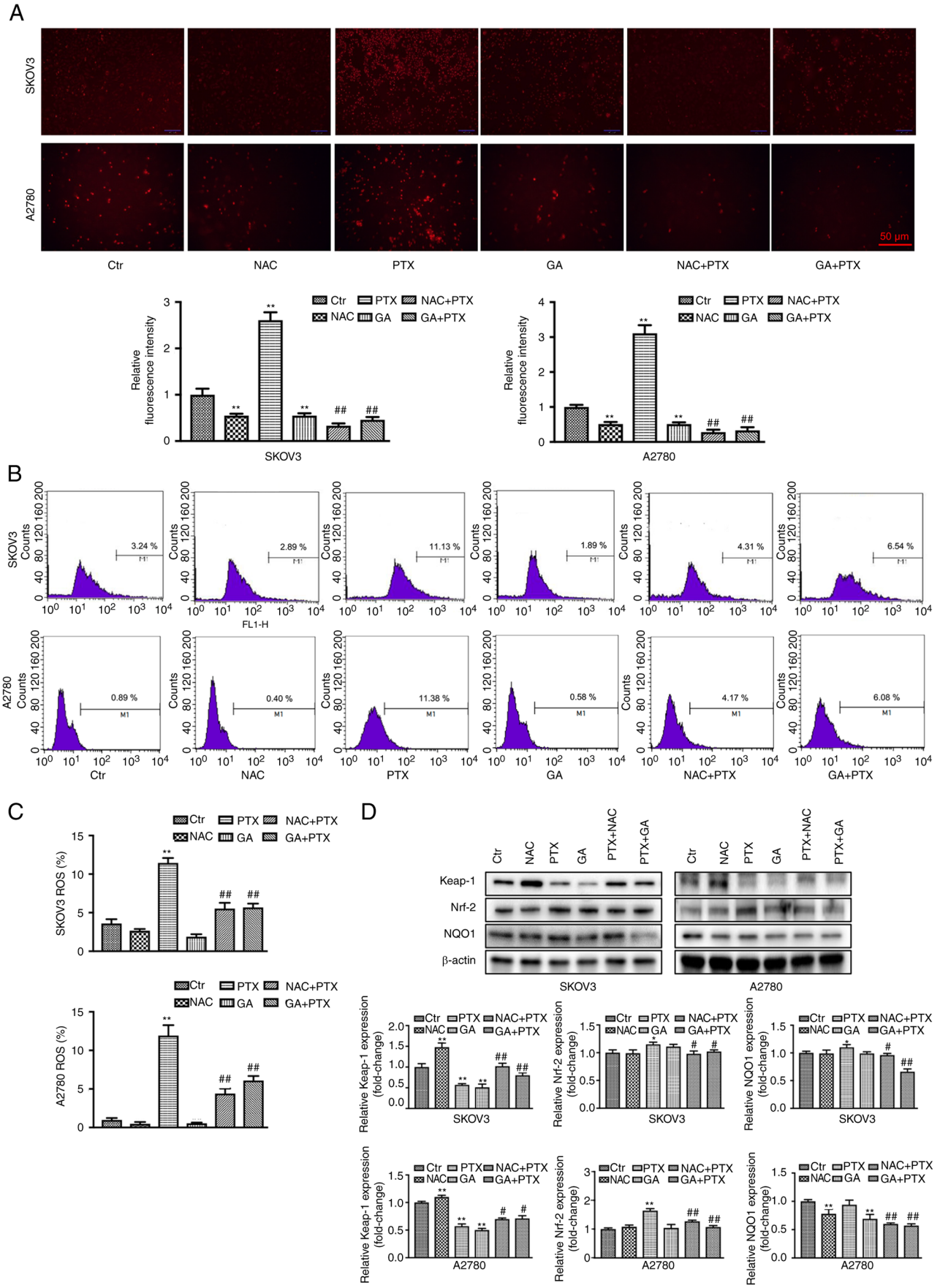

Figure 4. GA enhances the inhibitory effect of PTX by downregulating the levels of ROS. (A) DHE staining and statistical analysis of ROS in SKOV3 and A2780 cells following different treatments. (B and C) Flow cytometric and statistical analysis of ROS levels in SKOV3 and A2780 cells following different treatments, as determined by DCHF-DA staining. (D) Expression levels of Keap-1, Nrf-2 and NQO1, as detected by western blot analysis. Data are expressed as the mean ± SD from three independent experiments. *P<0.05, **P<0.01 vs. Ctrl; $^{\#}$P<0.05, $^{\#\#}$P<0.01 vs. PTX. Ctr, control; DHE, dihydroethidium; GA, Gomisin A; NAC, N-acetyl cysteine; PTX, paclitaxel; ROS, reactive oxygen species.

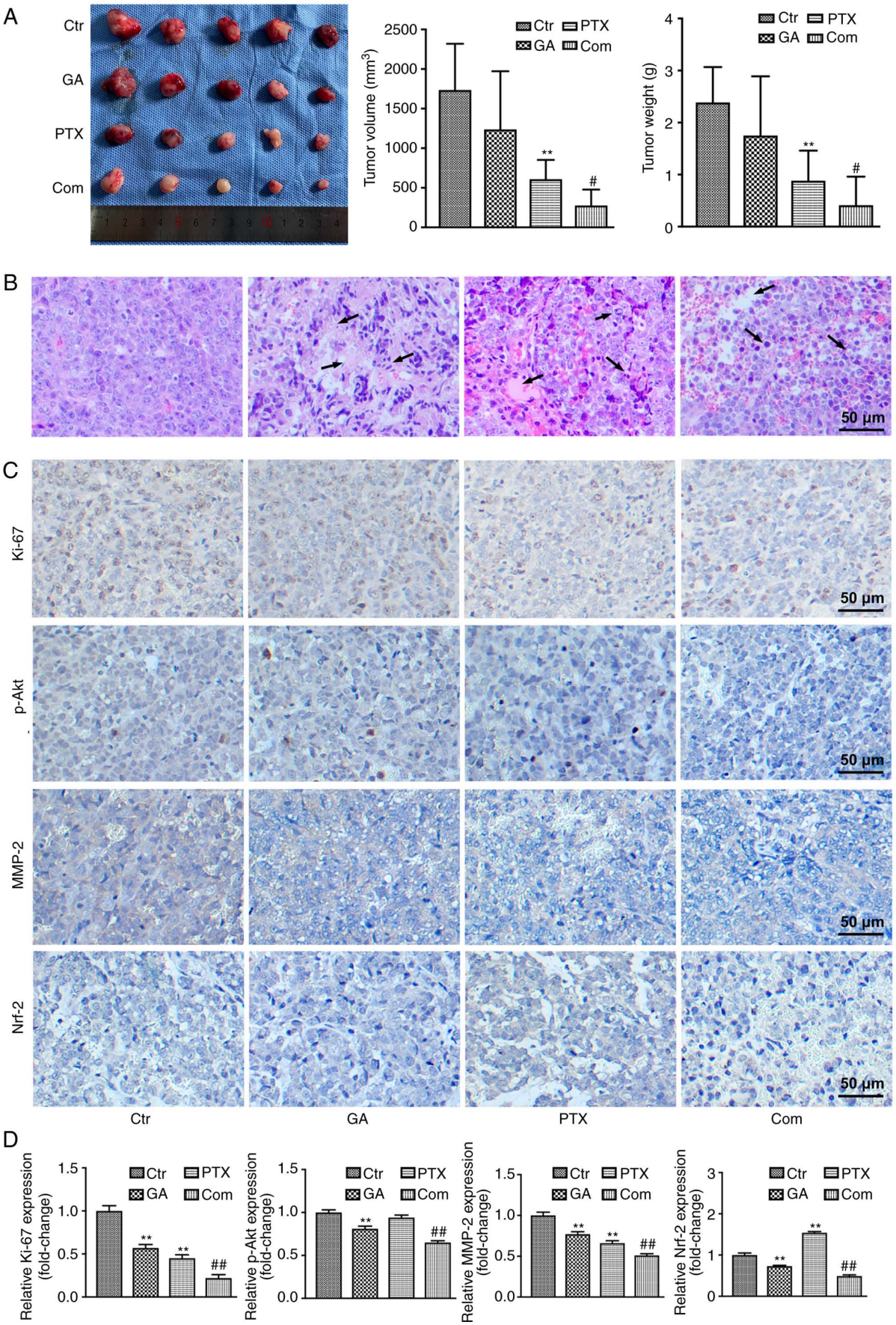

Figure 5. GA enhances the inhibitory effect of PTX on transplanted tumours. (A) Volume (left and middle panels) and weight (right panel of transplanted tumours. (B) H&E staining of transplanted tumours. H&E staining showed more tumour necrosis and the tumour tissue was impaired with nuclear pyknosis and fragmentation, with some nuclei disappearing (arrows), in the GA, PTX and combined groups compared with in the control group. (C) Immunohistochemical staining of Ki-67, p-Akt, MMP-2 and Nrf-2. (D) Semi-quantification of immunohistochemical staining analysis. **P<0.01 vs. Ctrl; $^{\#}$P<0.05, $^{\#\#}$P<0.01 vs. PTX, Ctr, control; Com, combined; GA, Gomisin A; p, phosphorylated; PTX, paclitaxel; MMP-2, matrix metallopeptidase 2; H&E, haematoxylin and eosin.

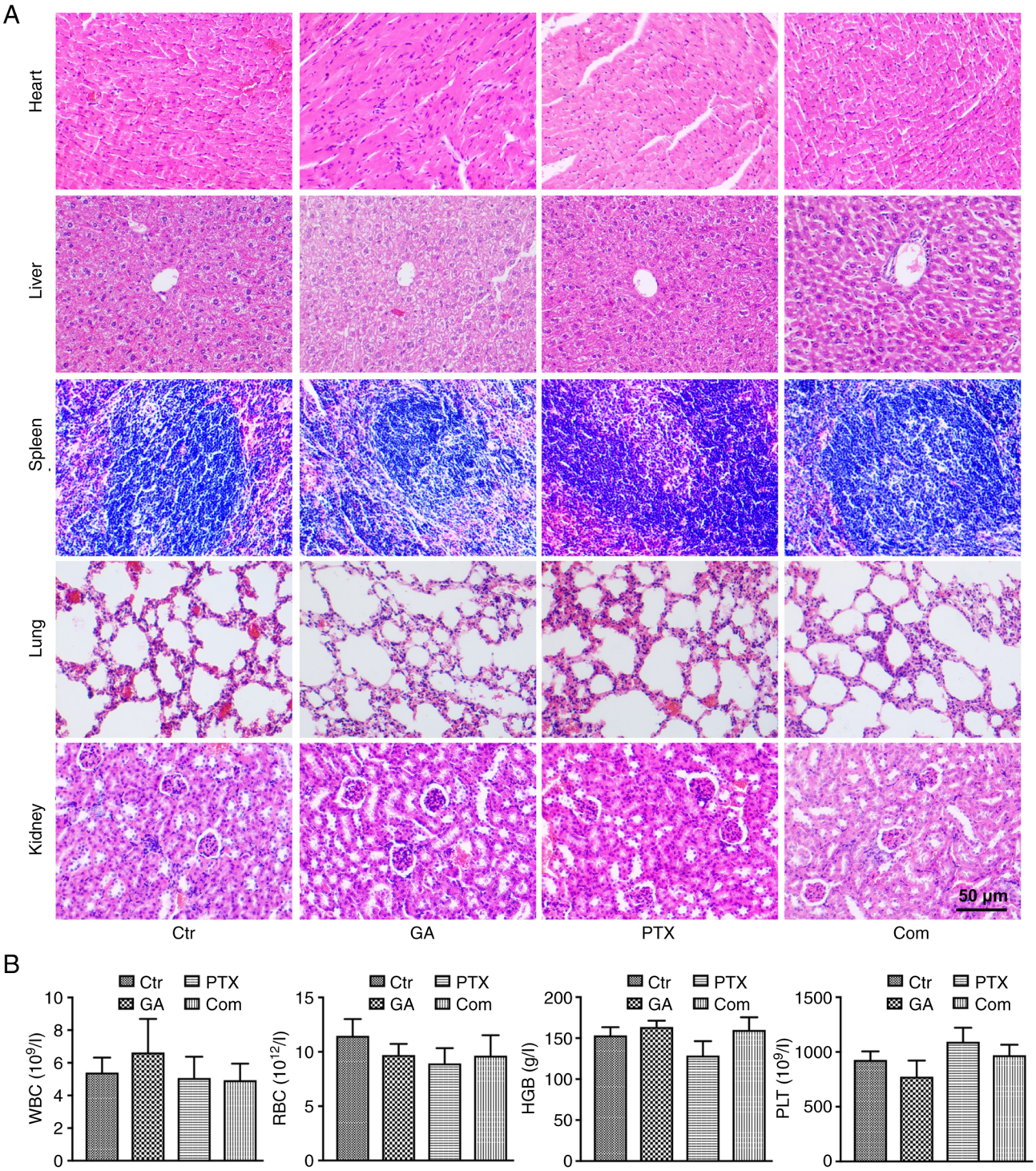

Figure 6. Biosafety assessments of GA and PTX treatments. (A) Haematoxylin and eosin staining of the histological changes in the heart, liver, spleen, lung and kidney. (B) Routine blood examinations of WBC, RBC, HGB and PLT counts. Ctr, control; GA, Gomisin A; Com, combined; HGB, haemoglobin; PLT,platelet; PTX, paclitaxel; RBC, red blood cell; WBC, white blood cell.

whereas low ROS concentrations promote cell survival (37). ROS may benefit therapeutic resistance in cancer (38). In most tumours, the high level of ROS production caused by chemotherapy or radiotherapy has been considered an antitumour factor (39); however, a low level of ROS is a key driver of tumour initiation. Immortal proliferation of cancer cells can be initiated by a low ROS environment that can regulate the cell cycle, autophagy and metastasis. Our previous study also reported that low levels of ROS could attenuate the antitumor effect of Raddeanin on SKOV3 cells (40). The detection of ROS implied that the levels of ROS in the GA + PTX group were significantly decreased compared with those in the PTX group, and the expression levels of Nrf-2 and NQO1 were downregulated, indicating that SKOV3 and A2780 cells were subjected to a lower degree of oxidative stress. These results suggested that low-dose ROS induced by PTX is one of the mechanisms limiting the tumour suppressive effect of PTX. Combining PTX with GA or NAC intensified

the antiproliferative effect of PTX, implying that the sensitivity of OC cells to PTX was heightened when the cells lost the irritation of low-level ROS, also suggesting that GA enhanced the sensitivity of A2780 and SKOV3 cells to PTX by inhibiting intracellular ROS generation.

To further explore the mechanism underlying the antitumour effect of GA combined with PTX on OC cells, apoptosis and proliferation were detected. Cell death via apoptosis is required for homeostatic turnover of cells under physiological conditions; however, it is usually inhibited in tumours. Thus, apoptosis has been regarded as an essential mechanism of antitumor effects in most treatment methods (41). In addition, the apoptosis-related signalling pathway, the PI3K/Akt pathway, was evaluated (42). The results of the present study are consistent with those of previous studies (43,44), showing that PTX can exert its antitumour effect by promoting cell apoptosis; however, there was no difference between PTX and the combined treatment in terms of cell apoptosis. PTX is a drug that inhibits mitosis (45). High doses of PTX have been reported to promote apoptosis (43,44). In the present study, low doses of PTX were used. Although the percentage of apoptotic cells detected in response to PTX was <10%, there was still a statistically significant difference between the PTX and control groups. In addition, low-dose ROS stimulation produced by PTX upregulated the expression of p-AKT, which was significantly downregulated following treatment with GA. This indicated that the PI3K/Akt pathway may be involved in the mechanism by which GA mediates the enhancement of sensitivity to PTX in OC cells. Subsequent studies should consider using a PI3K/Akt inhibitor as a positive control to further assess this.

In addition, the relationship between the PI3K/Akt pathway and the oxidative stress-related Keap1/Nrf-2 pathway has been extensively reported. Resveratrol has been shown to protect porcine intestinal epithelial cells from oxidative stress through the PI3K/Akt-mediated Nrf2 signalling pathway (46). The protective effect of *Chrysanthemum morifolium* on cell oxidative damage has also been reported to be related to the PI3K/Akt-mediated Nrf2/HO-1 signalling pathway (47). As an upstream signalling pathway, the PI3K/Akt pathway serves a key role in regulating Nrf-2/HO-1 protein expression. PI3K/Akt can dissociate Nrf-2 from Keap1 and promote subsequent signal transduction, thus inducing the activation of antioxidant enzymes.

It has previously been reported that ROS regulate tumours via multiple mechanisms, including apoptosis and the cell cycle (48). The cell cycle consists of mainly two phases, G_1/S and G_2/M, is essential for cell survival and is modulated by a stream of molecules. The two cell cycle phases are tightly controlled by cyclins, CDKs and CDK inhibitors. The present study revealed that PTX could inhibit A2780 and SKOV3 cells by inducing G_2/M phase arrest. Notably, the production of low levels of ROS could promote the cell cycle process (20), which was in accordance with the present finding that the ROS inhibitor GA or NAC could prolong the G_2/M phase arrest induced by PTX. CDKs are a group of serine/threonine protein kinases, which drive the cell cycle through the chemical action of serine/threonine proteins and act synergistically with cyclin, which is an important factor in cell cycle regulation. Among the CDK family members, CDK4 has an important role in regulating G_1 cells (27). Moreover, the decrease in cyclin B1 has been related to inactivation of the G_2/M checkpoint and G_2/M phase arrest (28). As cyclin B1/CDK1 can modulate mitochondrial activities in cell cycle progression and proliferation, subsequent studies will fully consider evaluating the expression of CDK1 to illustrate whether GA enhances the therapeutic effect of PTX through its effects on mitochondrial function.

All of these findings suggested that low levels of ROS may promote OC cell proliferation via a cell cycle mechanism and that the sensitivity of OC cells to PTX could be enhanced by the GA-induced reduction in ROS, which may further block the cell cycle compared with PTX alone. This model provides a strong strategy to target ROS with GA in OC therapy.

In conclusion, the present study showed that GA enhanced the inhibition rate of PTX by reducing the ROS levels in human OC cells both *in vivo* and *in vitro*. Furthermore, it was revealed that the mechanism was not related to the apoptosis pathway. However, G_2/M phase arrest was associated with the mechanism. The present findings suggested that the combination of GA and PTX may be a promising treatment for OC.

Acknowledgements

Not applicable.

Funding

This work was supported by grants from the Jilin Province of Department Finance (grant nos. 2019SCZT040 and 2019SCZT050) and the Jilin Province Science and Technology Department (grant no. 20200201589JC).

Availability of data and materials

The datasets used and/or analysed during the current study are available from the corresponding author on reasonable request.

Authors' contributions

SHZ, JL and TWW conceived and designed the experiments. TWW, CQZ, MYS, JYC and ZYY performed the experiments. XMH, MMC and SW analysed the data. XMH, SW, MMC and ZYY wrote the manuscript, critically revised the study for important intellectual content, and performed language editing. JL and SHZ supervised the study and were involved in project management. SHZ and TWW confirm the authenticity of all the raw data. All authors read and approved the final manuscript, and agree to be accountable for all aspects of the research in ensuring that the accuracy or integrity of any part of the work are appropriately investigated and resolved.

Ethics approval and consent to participate

The animal experiments were approved by the Institutional Animal Care and Use Committee of Jilin University Second Hospital.

Patient consent for publication

Not applicable.

Competing interests

The authors declare that they have no competing interests.

References

1. Merritt MA, Rice MS, Barnard ME, Hankinson SE, Matulonis UA, Poole EM and Tworoger SS: Pre-diagnosis and post-diagnosis use of common analgesics and ovarian cancer prognosis (NHS/NHSII): A cohort study. Lancet Oncol 19: 1107-1116, 2018.
2. Liu J and Matulonis UA: New strategies in ovarian cancer: Translating the molecular complexity of ovarian cancer into treatment advances. Clin Cancer Res 20: 5150-5156, 2014.
3. du Bois A, Kristensen G, Ray-Coquard I, Reuss A, Pignata S, Colombo N, Denison U, Vergote I, Del Campo JM, Ottevanger P, *et al*: Standard first-line chemotherapy with or without nintedanib for advanced ovarian cancer (AGO-OVAR12):A randomised,double-blind,placebo-controlled phase 3 trial. Lancet Oncol 17: 78-89, 2016.
4. Majidi A, Na R, Dixon-Suen S, Jordan SJ and Webb PM: Common medications and survival in women with ovarian cancer: A systematic review and meta-analysis. Gynecol Oncol 157: 678-685, 2020.
5. van der Hel OL, Timmermans M, van Altena AM, Kruitwagen RFPM, Slangen BFM, Sonke GS, van de Vijver KK and van der Aa MA: Overview of non-epithelial ovarian tumours: Incidence and survival in the Netherlands, 1989-2015. Eur J Cancer 118: 97-104, 2019.
6. Zierhut C, Yamaguchi N, Paredes M, Luo JD, Carroll T and Funabiki H: The cytoplasmic DNA sensor cGAS promotes mitotic cell death. Cell 178: 302-315.e23, 2019.
7. Koshiyama M, Matsumura N, Imai S, Yamanoi K, Abiko K, Yoshioka Y, Yamaguchi K, Hamanishi J, Baba T and Konishi I: Combination of aprepitant, azasetron, and dexamethasone as antiemetic prophylaxis in women with gynecologic cancers receiving paclitaxel/carboplatin therapy. Med Sci Monit 23: 826-833, 2017.
8. Ren F, Shen J, Shi H, Hornicek FJ, Kan Q and Duan Z: Novel mechanisms and approaches to overcome multidrug resistance in the treatment of ovarian cancer. Biochim Biophys Acta 1866: 266-275, 2016.
9. Li Z, He X, Liu F, Wang J and Feng J: A review of polysaccharides from *Schisandra chinensis* and *Schisandra* sphenanthera: Properties, functions and applications. Carbohydr Polym 184: 178-190, 2018.
10. Lv XJ, Zhao LJ, Hao YQ, Su ZZ, Li JY, Du YW and Zhang J: Schisandrin B inhibits the proliferation of human lung adenocarcinoma A549 cells by inducing cycle arrest and apoptosis. Int J Clin Exp Med 8: 6926-6936, 2015.
11. Xu Y, Liu Z, Sun J, Pan Q, Sun F, Yan Z and Hu X: Schisandrin B prevents doxorubicin-induced chronic cardiotoxicity and enhances its anticancer activity in vivo. PLoS One 6: e28335, 2011.
12. Chen Y, Shi S, Wang H, Li N, Su J, Chou G and Wang S: A Homogeneous polysaccharide from fructus *Schisandra chinensis* (Turz.) baill induces mitochondrial apoptosis through the Hsp90/AKT signalling pathway in HepG2 cells. Int J Mol Sci 17: 1015, 2016.
13. Chun JN, Cho M, So I and Jeon JH: The protective effects of *Schisandra chinensis* fruit extract and its lignans against cardiovascular disease: A review of the molecular mechanisms. Fitoterapia 97: 224-233, 2014.
14. Wan CK, Zhu GY, Shen XL, Chattopadhyay A, Dey S and Fong WF: Gomisin A alters substrate interaction and reverses P-glycoprotein-mediated multidrug resistance in HepG2-DR cells. Biochem Pharmacol 72: 824-837, 2006.
15. Young Park J, Wook Yun J, Whan Choi Y, Ung Bae J, Won Seo K, Jin Lee S, Youn Park S, Whan Hong K and Kim CD: Antihypertensive effect of gomisin A from *Schisandra chinensis* on angiotensin II-induced hypertension via preservation of nitric oxide bioavailability. Hypertens Res 35: 928-934, 2012.
16. Qu HM, Liu SJ and Zhang CY: Antitumor and antiangiogenic activity of *Schisandra chinensis* polysaccharide in a renal cell carcinoma model. Int J Biol Macromol 66: 52-56, 2014.
17. Han YH, Mun JG, Jeon HD, Park J, Kee JY and Hong SH: Gomisin A ameliorates metastatic melanoma by inhibiting AMPK and ERK/JNK-mediated cell survival and metastatic phenotypes. Phytomedicine 68: 153147, 2020.
18. Kee JY, Han YH, Mun JG, Park SH, Jeon HD and Hong SH: Gomisin A suppresses colorectal lung metastasis by inducing AMPK/p38-mediated apoptosis and decreasing metastatic abilities of colorectal cancer cells. Front Pharmacol 9: 986, 2018.
19. Alexandre J, Hu Y, Lu W, Pelicano H and Huang P: Novel action of paclitaxel against cancer cells: Bystander effect mediated by reactive oxygen species. Cancer Res 67: 3512-3517, 2007.
20. de Sá Junior PL, Câmara DAD, Porcacchia AS, Fonseca PMM, Jorge SD, Araldi RP and Ferreira AK: The roles of ROS in cancer heterogeneity and therapy. Oxid Med Cell Longev 2017: 2467940, 2017.
21. Harris IS and DeNicola GM: The complex interplay between antioxidants and ROS in cancer. Trends Cell Biol 30: 440-451, 2020.
22. Prasad S, Gupta SC and Tyagi AK: Reactive oxygen species (ROS) and cancer: Role of antioxidative nutraceuticals. Cancer Lett 387: 95-105, 2017.
23. Chen J, Liu J, Wu S, Liu W, Xia Y, Zhao J, Yang Y, Wang Y, Peng Y and Zhao S: Atrazine promoted epithelial ovarian cancer cells proliferation and metastasis by inducing low dose reactive oxygen species (ROS). Iran J Biotechnol 19: e2623, 2021.
24. Chen J, Xia Y, Peng Y, Wu S, Liu W, Zhang H, Wang T, Yang Z, Zhao S and Zhao L: Analysis of the association between KIN17 expression and the clinical features/prognosis of epithelial ovarian cancer, and the effects of KIN17 in SKOV3 cells. Oncol Lett 21: 475, 2021.
25. Zeng Z, Wang Q, Yang X, Ren Y, Jiao S, Zhu Q, Guo D, Xia K, Wang Y, Li C and Wang W: Qishen granule attenuates cardiac fibrosis by regulating TGF-β/Smad3 and GSK-3β pathway. Phytomedicine 62: 152949, 2019.
26. Takanche JS, Kim JE, Han SH and Yi HK: Effect of gomisin A on osteoblast differentiation in high glucose-mediated oxidative stress. Phytomedicine 66: 153107, 2020.
27. Goel S, DeCristo MJ, Watt AC, BrinJones H, Sceneay J, Li BB, Khan N, Ubellacker JM, Xie S, Metzger-Filho O, *et al*: CDK4/6 inhibition triggers anti-tumour immunity. Nature 548: 471-475, 2017.
28. Jiang B, Ni H, Zhou Z and Li Y: Parkin enhances sensitivity of paclitaxel to NPC by arresting cell cycle. Pathol Res Pract 216: 152755, 2020.
29. Ahn JH, Lee HS, Lee JS, Lee YS, Park JL, Kim SY, Hwang JA, Kunkeaw N, Jung SY, Kim TJ, *et al*: nc886 is induced by TGF-β and suppresses the microRNA pathway in ovarian cancer. Nat Commun 9: 1166, 2018.
30. Han YH, Kee JY and Hong SH: Gomisin A alleviates obesity by regulating the phenotypic switch between white and brown adipocytes. Am J Chin Med 49: 1929-1948, 2021.
31. Hao LJ, Lin RA, Chen LC, Wang JL, Chen IS, Kuo CC, Chou CT, Chien JM and Jan CR: Action of the natural compound gomisin a on Ca^{2+} movement in human prostate cancer cells. Chin J Physiol 65: 151-157, 2022.
32. da Cunha Santos G, Shepherd FA and Tsao MS: EGFR mutations and lung cancer. Annu Rev Pathol 6: 49-69, 2011.
33. Talukdar S, Emdad L, Das SK and Fisher PB: EGFR: An essential receptor tyrosine kinase-regulator of cancer stem cells. Adv Cancer Res 147: 161-188, 2020.
34. Ko YH, Jeong M, Jang DS and Choi JH: Gomisin L1, a lignan isolated from *Schisandra* berries, induces apoptosis by regulating NADPH oxidase in human ovarian cancer cells. Life (Basel) 11: 858, 2021.
35. Kretzmann NA, Chiela E, Matte U, Marroni N and Marroni CA: N-acetylcysteine improves antitumoural response of Interferon alpha by NF-kB downregulation in liver cancer cells. Comp Hepatol 11: 4, 2012.
36. Liu B, Huang X, Li Y, Liao W, Li M, Liu Y, He R, Feng D, Zhu R and Kurihara H: JS-K, a nitric oxide donor, induces autophagy as a complementary mechanism inhibiting ovarian cancer. BMC Cancer 19: 645, 2019.
37. Mendes S, Sá R, Magalhães M, Marques F, Sousa M and Silva E: The role of ROS as a double-edged sword in (In)Fertility: The impact of cancer treatment. Cancers (Basel) 14: 1585, 2022.

38. Okon IS and Zou MH: Mitochondrial ROS and cancer drug resistance: Implications for therapy. Pharmacol Res 100: 170-174, 2015.
39. Ma N, Liu P, He N, Gu N, Wu FG and Chen Z: Action of gold nanospikes-based nanoradiosensitizers: Cellular internalization, radiotherapy, and autophagy. ACS Appl Mater Interfaces 9: 31526-31542, 2017.
40. Zhao F, Gao Y, Chu X, Chen J, Huang L, Zhao J, Zhang J and Zhao S: ROS attenuates the antitumor effect of Raddeanin on ovarian cancer cells Skov3. Int J Clin Exp Pathol 10: 8292-8302, 2017.
41. Wong RS: Apoptosis in cancer: From pathogenesis to treatment. J Exp Clin Cancer Res 30: 87, 2011.
42. Jiang S, Zhang E, Ruan H, Ma J, Zhao X, Zhu Y, Xie X, Han N, Li J, Zhang H, *et al*: Actinomycin V induces apoptosis associated with mitochondrial and PI3K/AKT pathways in human CRC cells. Mar Drugs 19: 599, 2021.
43. Wang TH, Wang HS and Soong YK: Paclitaxel-induced cell death: Where the cell cycle and apoptosis come together. Cancer 88: 2619-2628, 2000.
44. Zhang CC, Li CG, Wang YF, Xu LH, He XH, Zeng QZ, Zeng CY, Mai FY, Hu B and Ouyang DY: Chemotherapeutic paclitaxel and cisplatin differentially induce pyroptosis in A549 lung cancer cells via caspase-3/GSDME activation. Apoptosis 24: 312-325, 2019.
45. Manfredi JJ and Horwitz SB: Taxol: An antimitotic agent with a new mechanism of action. Pharmacol Ther 25: 83-125, 1984.
46. Zhuang Y, Wu H, Wang X, He J, He S and Yin Y: Resveratrol attenuates oxidative stress-induced intestinal barrier injury through PI3K/Akt-mediated Nrf2 signaling pathway. Oxid Med Cell Longev 2019: 7591840, 2019.
47. Hao Y, Li Y, Liu J, Wang Z, Gao B, Zhang Y and Wang J: Protective effect of *Chrysanthemum morifolium* cv. Fubaiju hot-water extracts against ARPE-19 cell oxidative damage by activating PI3K/Akt-mediated Nrf2/HO-1 signaling pathway. Front Nutr 8: 648973, 2021.
48. Ren Y, Geng R, Lu Q, Tan X, Rao R, Zhou H, Yang X and Liu W: Involvement of TGF-β and ROS in G1 cell cycle arrest induced by titanium dioxide nanoparticles under UVA irradiation in a 3D spheroid model. Int J Nanomedicine 15: 1997-2010, 2020.